Permeability and Diffusion in Vitreous Humor: Implications for Drug Delivery

Jing Xu,[1] Jeffrey J. Heys,[1] Victor H. Barocas,[1] and Theodore W. Randolph[1,2]

Received January 10, 2000; accepted February 23, 2000

Purpose. Previous experimental work suggests that convection may be important in determining the biodistribution of drugs implanted or injected in the vitreous humor. To develop accurate biodistribution models, the relative importance of diffusion and convection in intravitreal transport must be assessed. This requires knowledge of both the diffusivity of candidate drugs and the hydraulic conductivity of the vitreous humor.

Methods. Hydraulic conductivity of cadaveric bovine vitreous humor was measured by confined compression tests at constant loads of 0.15 and 0.2 N and analyzed numerically using a two-phase model. Diffusion coefficient of acid orange 8, a model compound, in the same medium was measured in a custom-built diffusion cell.

Results. Acid orange 8 diffusivity within vitreous humor is about half that in free solution. When viscous effects are properly accounted for, the hydraulic conductivity of bovine vitreous humor is $8.4 \pm 4.5 \times 10^{-7}$ cm^2/Pa · s.

Conclusions. We predict that convection does not contribute significantly to transport in the mouse eye, particularly for low-molecular-weight compounds. For delivery to larger animals, such as humans we conclude that convection accounts for roughly 30% of the total intravitreal drug transport. This effect should be magnified for higher-molecular-weight compounds, which diffuse more slowly, and in glaucoma, which involves higher intraocular pressure and thus potentially faster convective flow. Thus, caution should be exercised in the extrapolation of small-animal-model biodistribution data to human scale.

KEY WORDS: controlled drug delivery; permeability.

INTRODUCTION

Although topical application of drugs to the eye is often the most convenient route of delivery, the small volume of the tear film, in addition to rapid clearance by the tear film and the aqueous humor, limits delivery to the retina and vitreous humor. The blood-retinal barrier (1) limits the accessibility of the vitreous and retina to systemic treatments. In response to these challenges, direct intravitreal injection of drug or controlled drug source has emerged as an alternative to traditional treatment methods (2–4). The vitreous humor (or simply "vitreous") is the clear, avascular, gelatinous body that fills the large space bounded by the lens, ciliary body, aqueous humor, and retina in the eye. Because it is large, relatively stagnant, and offers easy access to the retina, the vitreous is an attractive site for bolus or controlled-release delivery of therapeutic drugs for diseases such as proliferative vitreoretinopathy and endophthalmitis (5,6). Predicting transport of drug within the vitreous, however, requires us to understand the nature of and the interaction among the various processes that can occur within the vitreous.

Most previous work on transport in the vitreous has focused on diffusion, using fluorescein as a model compound. Nishimura *et al.* (7) derived a diffusion coefficient of 4.8×10^{-6} cm^2/s, and Kaiser and Maurice (8) measured a value of 6.0×10^{-6} cm^2/s. Kaiser and Maurice estimated the diffusion coefficient of fluorescein in free aqueous solution to be $5.7–6.0 \times 10^{-6}$ cm^2/s, suggesting relatively little hindrance of fluorescein diffusion by the vitreous. Ohtori and Toko (9) designed an apparatus to measure drug diffusion in the vitreous humor. They found the diffusion coefficient for dexamethasone sodium m-sulfobenzoate to be 5.1×10^{-6} cm^2/s, about 30% lower than the respective diffusion coefficient in aqueous solution.

Mass transport in the vitreous humor is caused by both diffusion and convection. Convection arises because of steady permeating flow through the vitreous driven by a pressure drop between the anterior (hyaloid membrane) and the posterior (retina) surfaces and/or by active transport through the retinal pigment epithelium (10). Permeation is generally described by Darcy's Law:

$$v_{fluid} = -\frac{K}{\mu_{fluid}} \nabla P \qquad (1)$$

where v_{fluid} is the velocity of the permeating fluid, K is the hydraulic conductivity of the vitreous, μ_{fluid} is the viscosity of permeating fluid, and ∇P is the gradient of pressure. Because pressure drops across the vitreous are low, and K/μ_{fluid} is presumed to be small, diffusion has generally been regarded as the primary mechanism for drug transport within the vitreous (9,11,12). There is, however, a body of evidence (13–16) suggesting that convection by intravitreal flow may be significant. In particular, vitreal flows may be important in pathological states (e.g., glaucoma) or in controlled-release applications of therapeutic agents where precise dosage and targeting are required (e.g., anti-cancer agents). In order to assess the importance of intravitreal flow, one must measure the hydraulic conductivity of the vitreous; unfortunately, the softness and compressibility of the vitreous hinder attempts to make and interpret a direct conductivity measurement (14,17).

The hydraulic conductivity K/μ_{fluid}, defined as the hydraulic conductivity through the vitreous humor divided by the viscosity of the permeating liquid (generally assumed to be buffered saline solution), is needed to describe the convective transport. Fatt (17) determined hydraulic conductivity of bovine and rabbit vitreous by pneumatically compressing the respective vitreous humors and measuring the rate of water exudation. Reported bovine vitreous hydraulic conductivity values were $9 \pm 3 \times 10^{-8}$ cm^2/(Pa · s), with similar values for rabbit. These early attempts provided insight into intravitreal transport, but

[1] Department of Chemical Engineering, University of Colorado, Boulder, Colorado 80309-0424.

[2] To whom correspondence should be addressed. (e-mail: randolph@pressure3.colorado.edu)

ABBREVIATIONS: A, area (cm^2); c, concentration (mg/cm^3); D, diffusion coefficient (cm^2/s); k, mass transfer coefficient (cm/s); K, hydraulic conductivity (cm^2); $K_{VH/W}$, partition coefficient between vitreous humor and water (−); L, length (cm); MW, molecular weight (g/mol); P, pressure (Pa); Pe, Peclet Number (−); v, velocity (cm/s); η, confined compression viscosity (Pa · s); μ_{fluid}, viscosity of permeating fluid (Pa · s); θ, network volume fraction.

0724-8741/00/0600-0664$18.00/0 © 2000 Plenum Publishing Corporation

they failed to account for the viscosity of the vitreous or for nonuniform compaction of the vitreous during compression experiments.

Detailed models of intravitreal transport are needed to interpret pharmacokinetic and pharmacodynamic data for drug delivery to the vitreous. Both experimental measurements of transport properties and computationally efficient three-dimensional models must be obtained. In this manuscript, we address experimental techniques and analyses required to generate transport properties, using cadaveric bovine vitreous as a model system and acid orange 8 as a model diffusant.

MATERIALS AND METHODS

Materials and Analysis

Vitreous humor was dissected from bovine eyes (Monford Biological; Greeley, CO); the protocol for animal cadaveric material was approved according to relevant laws and institutional regulations. Each experiment used vitreous from an individual eye. Acid orange 8 (AO8, dye content approx. 85%, average MW 364.4) was purchased from Sigma Chemical Co. (St. Louis, MO). The concentration of AO8 solution was determined using a UV-visible spectrophotometer (Hewlett-Packard; Palo Alto, CA); absorbance was measured at 492 nm.

Diffusion Coefficient—Experiment

The diffusion cell shown in Fig. 1 was constructed to measure the diffusion coefficient of AO8 in the vitreous humor. Two reservoirs were separated by a slab of vitreous held between two porous stainless steel plates. The thickness of each porous stainless steel plate was 0.23 cm, the diameter was 4.22 cm, and the pore diameter was 100 μm. The height of the vitreous layer between the two stainless steel plates was 0.5 cm. The upper reservoir was filled with phosphate-buffered saline solution (PBS) containing a high concentration of AO8, and the lower reservoir was filled with drug-free PBS at the beginning of the experiments. The upper reservoir was narrower than the lower one to eliminate edge bypass effects arising when the vitreous sample did not completely fill the space between the plates. Over time, AO8 diffused through the porous plates and vitreous and subsequently entered the lower reservoir. Samples, 1 ml each time, were taken periodically from the sample port in the lower reservoir while fresh buffer solution was added to maintain constant reservoir volume.

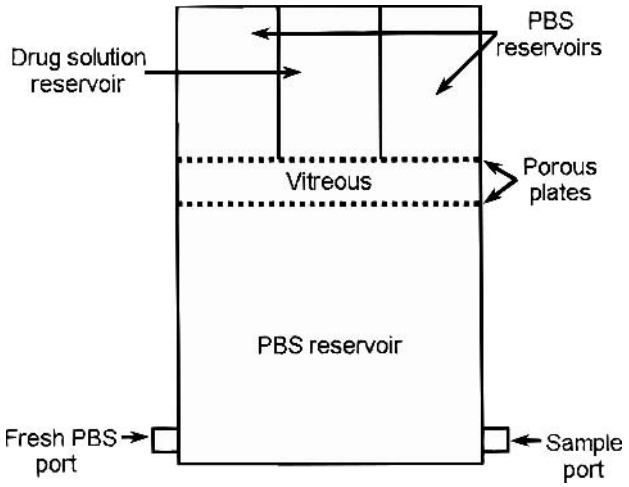

Fig. 1. Diffusion Cell. The diffusion cell was specially designed with the upper (high dye concentration) reservoir narrower than the vitreous sample to prevent leakage around the sample edge. Samples were taken periodically through the sample port, and an equal volume of PBS was simultaneously added to avoid suction into the lower chamber. Care was taken to remove all air from upper chamber so as to prevent convective flow from the upper to the lower chamber during sampling. The lower sink container is stirred.

The analysis of the diffusion experiments (see below) requires the equilibrium partition coefficient of AO8 between water and vitreous ($K_{VH/W}$, defined as the ratio of concentration in vitreous to concentration in PBS). To obtain this, we incubated samples of vitreous suspended in PBS containing initial AO8 concentrations of 5–50 μM until no concentration change was observed. Final concentrations of AO8 in the medium and the vitreous were plotted, and linear regression gave a partition coefficient of 1.60 ± 0.07 ($r^2 = 0.94$; N.B. ± values in this paper refer to 95 % confidence limits). This slight preference of AO8 for the vitreous was consistent with visual observation of faint staining of the vitreous by the AO8.

Diffusion Coefficient—Model and Data Analysis

Once quasi-steady diffusion had been attained, the flux was constant across the vitreous and the support plates and was described by the following expression:

$$\text{Mass transferred per unit time} = Ak\Delta c$$

where A is the area available for transport, k is a mass transfer coefficient, and Δc is the concentration difference between the upper and lower compartments. For steady Fickian diffusion through a series of slabs, it is well established that:

$$\frac{1}{kA} = \frac{L}{D_{VH} \cdot K_{VH/W} \cdot A} + \frac{2L_M}{D_M \cdot A_M} \qquad (2)$$

where L_M is the thickness of the metal plate (the factor of 2 appears because there are two plates, one above and one below the sample), L is the thickness of the sample (vitreous humor in this case), D_M is the diffusion coefficient in the pores of the plate, A_M is the total pore area of the metal plate, and D_{VH} is the diffusion coefficient in the vitreous humor. $K_{VH/W}$ is the partition coefficient defined above.

We assumed that the pores of the plates were filled with PBS, so D_M was taken to be equal to D_W (diffusion coefficient in water). The other unknown parameter in Eq. (2) was the value of the ratio L_M/A_M. This value was estimated by repeating the experiment with PBS instead of vitreous between the plates. When we replaced the vitreous humor with water, a new mass transfer coefficient, k_W, was obtained. The same consecutive-slab model gives:

$$\frac{1}{k_W A} = \frac{1}{D_W}\left(\frac{2L_M}{A_M} + \frac{L}{A}\right) \qquad (3)$$

Since everything else was known, equation (3) allowed calculation of the ratio L_M/A_M. Once that had been determined from the water-only experiments, equation (2) and the vitreous humor experiments were used to calculate the diffusivity of solutes in the vitreous.

Hydraulic Conductivity—Confined Compression Experiments

The ratio K/μ_{fluid}, defined as the hydraulic conductivity, was measured by confined compression as shown in Fig. 2 (cf. (18,19)). In the experiment, bovine vitreous humor was placed in an impermeable cup and compressed by a polyethylene piston with high porosity. The vitreous humor and solution flows were confined by the side of the cup, so the deformation could be regarded as occurring only in the axial direction. The tests were conducted on a Minimat 2000 Miniature Materials Tester (Rheometric Scientific; Piscataway, NJ), which allowed simultaneous measurement of the force applied to the piston and its displacement.

We performed a series of creep experiments, in which a constant compressive force was applied, and the displacement of the piston was recorded. Creep tests were performed for applied loads of 0.15 and 0.20 N. Since the cross-sectional area of our system is 0.0011 m^2 (37 mm diameter), these loads correspond to stresses of 140 and 190 Pa, respectively. Initial sample length varied between 2 and 5 mm. The confined compression system was kept at 37°C and submerged in PBS during the experiments.

Hydraulic Conductivity—Model and Data Analysis

Because the vitreous humor is compressible as well as permeable to water (20–22), experimental determination of the hydraulic conductivity requires separation of the coupled permeation and deformation phenomena. In order to describe the complex response of the vitreous gel, we adapted an averaging-theory description of collagen gel (18,23). This theory treats the gel as two coexisting phases, a viscoelastic fluid network phase (representing the collagen and hyaluronic acid in the vitreous) and a permeating solution phase (water and drug).

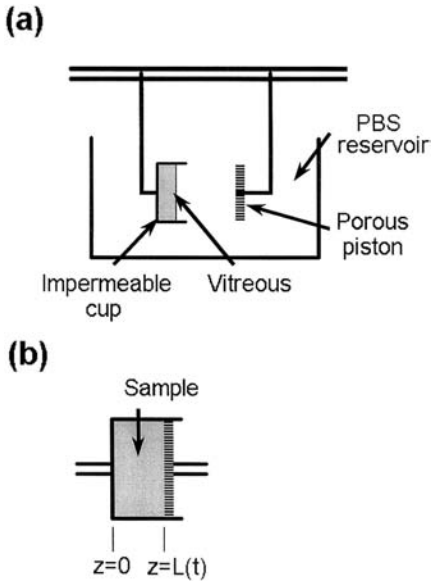

Fig. 2. Confined Compression. (a) Confined compression experiments were performed by placing a sample of vitreous gel in an impermeable cup and compressing it with a porous piston. The entire sample was maintained in a 37°C PBS bath. (b) The compression system is one-dimensional with the sample length changing as a function of time.

Because of the extreme fluidity of the vitreous, we removed the elastic term from the model, and treated the vitreous as a two-phase mixture: the compressible, viscous network phase and the macroscopically inviscid (i.e., resistant to permeation but not to macroscopic flow) water phase (cf. (24)).

The confined compression test is assumed to be one-dimensional, so considerable simplification of the model equations was possible. The conservation of mass equation is

$$\dot{\theta} = -\theta \frac{dv}{dz} \tag{4}$$

where θ and v are the network phase volume fraction and velocity. The dot denotes the material derivative moving with the network. As described earlier, we used a compressible Newtonian fluid model for the network phase, which leads to the following modified form of the equations of (18):

$$\frac{d}{dz}\left(\eta\theta \frac{\partial v}{\partial z}\right) - \frac{1}{(1-\theta)^2(K/\mu_{fluid})} v = 0 \tag{5}$$

in which η is the aggregate viscosity for confined compression, which is related to the shear viscosity by a transient Poisson's ratio, and K/μ_{fluid} is the hydraulic conductivity defined in (1). The $(1-\theta)^2$ term in (5), which arises from the averaging theory (24), accounts for decreased conductivity due to compression of the network.

The boundary conditions at $z = 0$ (the bottom of the impermeable cup, Fig. 2b) were no displacement of the vitreous ($v = 0$) and no permeation ($dP/dz = 0$). At $z = L(t)$, (the porous piston), the stress was specified to be that applied by the piston. The pressure was set to zero at the piston (no resistance to permeation). The initial conditions were no displacement and uniform distribution of network.

There is no known analytical solution to the nonlinear partial differential equation system (4)–(5), so a numerical solution was obtained by the method of lines. The Standard Galerkin finite element method was used to convert the partial differential equations into ordinary differential equations. This ODE system was then solved numerically using the COOPT program (25). In addition to solving the model equations, COOPT allows optimization of model parameters to minimize a given objective function. By defining the objective function to be the sum of squared error between the model prediction and the experimental result, we used COOPT to regress η and K/μ_{fluid}.

RESULTS AND DISCUSSION

Diffusion Coefficient

In order to use equations (2) and (3) to determine AO8 diffusivity in vitreous, we needed to know the diffusion coefficient for AO8 in water. Since that value was not available from published literature, an estimate was made based on sucrose, which is of similar molecular weight (342.2 vs. 364.4). The diffusion coefficient of sucrose in water is known to be 6.8×10^{-6} cm^2/s (26). Using the Wilke-Chang correlation and assuming that the molar volume of each species at its normal boiling point is proportional to its molecular weight leads to the following expression:

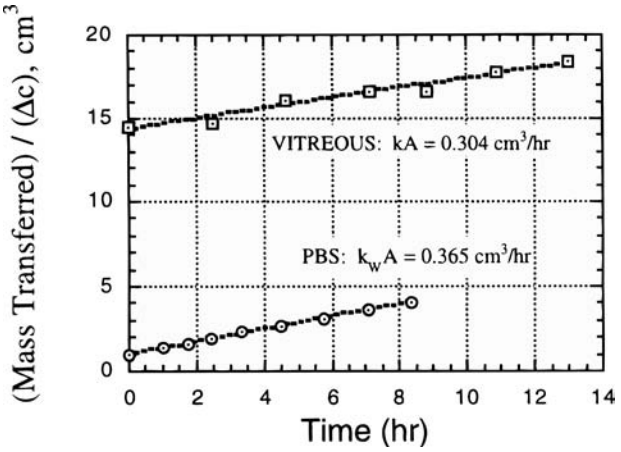

Fig. 3. Diffusion of Acid Orange 8 through PBS and Vitreous. The plot shows the accumulation of AO8 in the lower chamber of the diffusion cell. The time axis is normalized so that t = 0 represents the start of steady diffusion across the cell.

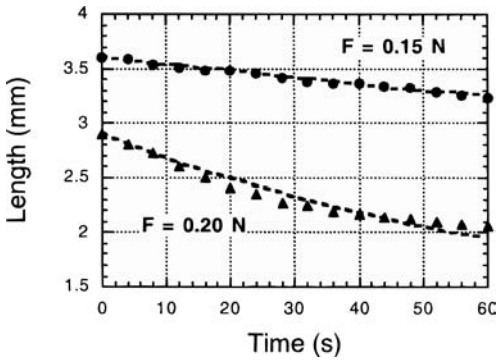

Fig. 4. Typical Creep Results. Two creep experiments (solid symbols) with the corresponding model fits (dashed lines) are shown. For the 0.15 N experiment, the best-fit model parameters were $\eta = 2.8 \times 10^4$ Pa · s and $K/\mu_{fluid} = 6.5 \times 10^{-7}$ cm^2/(Pa · s). For the 0.2 N experiment, the best-fit model parameters were $\eta = 3.0 \times 10^4$ Pa · s and $K/\mu_{fluid} = 5.8 \times 10^{-7}$ cm^2/(Pa · s).

$$\frac{D_{AO8}}{D_{sucrose}} = \left(\frac{MW_{sucrose}}{MW_{AO8}}\right)^{0.6}$$

which yields a diffusion coefficient of 6.5×10^{-6} cm^2/s for AO8 in water.

Typical results for diffusion experiments with and without vitreous present are shown in Fig. 3; the slope of each line was used in conjunction with (3) to determine the overall mass transfer coefficient. Based on the data, we calculated $D_{VH} = 3.4 \pm 0.2 \times 10^{-6}$ cm^2/s. The diffusion coefficient of AO8 in vitreous humor was thus about 50% lower than that in aqueous solution.

Although no published data on AO8 diffusion in vitreous are available, there are a number of relevant studies to which we can compare our results. The diffusion coefficient of a similarly sized azo dye (dye #2 in (27)) in gelatin (10-20% protein content) was found to obey the law $\log(D) \sim \alpha_0 - \alpha_1/(1 - \theta)$, where α_0 and α_1 are constants, and θ is the volume fraction of protein in the gel. Applying that model to our system yields the result that the diffusion coefficient is 50% lower than that in water for a gel with 6% protein. Although the vitreous is less than 1% total organics, this result is reasonable in light of the fact that hyaluronic acid hydrates significantly and thus has a very high effective concentration (1).

Ohtori and Toko obtained the diffusion coefficient for dexamethasone sodium *m*-sulfobenzoate (DMSB) in vitreous using an apparatus similar to ours and an assumed partition coefficient of 1 in their analysis. The diffusion coefficients of DMSB were 7.0×10^{-6} cm^2/s in PBS and 5.1×10^{-6} cm^2/s in vitreous, corresponding to a 27% decrease in diffusivity.

Table 1 summarizes the results of this and previous studies. One would expect the diffusion coefficients of larger molecules to be more sensitive to the change from PBS to vitreous, but we observed a more dramatic drop for AO8 (MW 364) than Ohtori and Toko did for DMSB (MW ~ 600). The simplest explanation for this difference is that our calculation of diffusivity was based on a partition coefficient of 1.6 while the previous study did not account for partitioning (equivalent to a partition coefficient of 1 in our model). Since the calculated diffusion coefficient is inversely proportional to the partition coefficient, had we neglected the partition coefficient, we would have estimated a diffusion coefficient of 5.4×10^{-6} cm^2/s, corresponding to a 15% reduction from the PBS value and consistent with the expectation that retardation of diffusivity would increase with molecular size.

Hydraulic Conductivity

Representative creep test data and model fits for 0.15 and 0.2 N experiments are shown in Fig. 4, and the overall experimental results are summarized in Fig. 5. The model describes the experimental data quite well, but may be underpredicting the effect of compression on effective mechanical properties of the gel, as indicated by the slightly greater curvature in the experimental results than in the model fit. For a total of 14 experiments, we calculated an average hydraulic conductivity of $8.4 \pm 4.5 \times 10^{-7}$ cm^2/Pa · s with no significant difference between the different creep experiments (0.15 vs. 0.2 N). The viscosity was $3.4 \pm 1.4\ 10^4$ Pa · s, also with no significant difference between results for different loads. The approximate 95% confidence range on the parameter values from each regression fit was within ± 5%, indicating that variation between experiments was much greater than regression error.

Table 1. Diffusivity Measurements in Water and in Vitreous Gel

Compound	MW (g/mol)	Diffusivity in Water (10^{-6} cm^2/s)	Diffusivity in Vitreous (10^{-6} cm^2/s)	% Change	Source
Fluorescein	332.3	6.0	4.8–6.0	10	(7,8)
AO8	364.4	6.5	3.4	48	This study
DMSB	~600	7.0	5.1	27	(9)

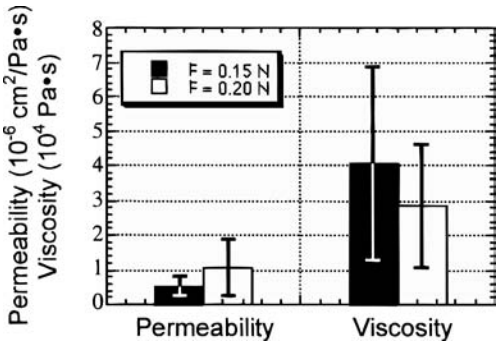

Fig. 5. Creep Results. A comparison of the results from the 0.15 N and the 0.2 N creep tests shows that there was a slight increase in measured hydraulic conductivity and a slight decrease in viscosity. Neither change was significant at the 90% confidence level.

Our mean measured hydraulic conductivity was somewhat higher than that reported by Fatt (17). One reason for the difference between the two values is that Fatt did not account for viscous resistance to compaction by the gel itself. As a result, his analysis attributed all flow resistance to permeation resistance and led to the calculation of a significantly underestimated hydraulic conductivity. If we ignored viscosity of the gel and applied Fatt's analysis to our data, we would calculate a hydraulic conductivity of $5.4 \pm 1.7 \times 10^{-7}$ cm^2/Pa · s, closer to Fatt's result.

Implications for Drug Delivery

In order to design effective drug delivery systems, especially controlled-release systems, one must be able to predict the destination of the drug once it has been released into the tissue. The standard approach to this problem has been to treat diffusion as the dominant mechanism for drug transport and to ignore convection by intravitreal flow. Using the vitreous conductivity measured in this study and published values for the conductivity and thickness of the sclera (28), we can estimate the flow rate of water through the vitreous. The pressure at the anterior surface of the vitreous is roughly 15 mm Hg in healthy eyes (1), and the pressure on the posterior surface of the sclera is close to zero (4). Fatt and Hedbys (28) reported a scleral conductivity K_{sc} of 1.5×10^{-11} cm^2/Pa · s and a scleral thickness L_{sc} of 0.03 cm. Using these data in conjunction with our measured data and a resistance-in-series flow model, we can write

$$v = \frac{\Delta P}{\left(\frac{L_{VH}}{K_{VH}} + \frac{L_{sc}}{K_{sc}}\right)} = \frac{2000\ \text{Pa}}{\left(\frac{1.4\ \text{cm}}{2.4 \times 10^{-6}\ \text{cm}^2/\text{Pa} - \text{s}} + \frac{0.03\ \text{cm}}{1.5 \times 10^{-11}\ \text{cm}^2/\text{Pa} - \text{s}}\right)} = 10^{-6}\ \text{cm/s}$$

and we can observe that, as Fatt and Hedbys suggested, the flow resistance in the sclera dominates the fluid mechanics even though the vitreous is much larger. Using the velocity calculated above, the diffusivity measured earlier, and a characteristic vitreous length scale of 1.4 cm (12), we can calculate a Peclet number for mass transport of

$$\acute{Pe}_{HUMAN} = \frac{vL}{D} = \frac{10^{-6}\ \text{cm/s} \cdot 1.4\ \text{cm}}{3.4 \times 10^{-6}\ \text{cm}^2/\text{s}} = 0.41$$

This suggests that even for a relatively small (and thus highly diffusive) molecule, such as acid orange 8, the contribution of convection to transport is not insignificant (roughly 40% of the diffusive contribution or, equivalently, roughly 30% of the total) and should be considered in designing delivery systems.

The consideration of convective transport is particularly important in the scale-up of treatments. Many drugs are tested in small animal models, for which convection becomes insignificant. The neonatal mouse eye, a common model system, is much smaller than the human, with a characteristic length scale of only 0.08 cm (29). Using this value for the length scale and assuming little species variation in the other parameters gives a mouse Peclet number of

$$\acute{Pe}_{MOUSE} = \frac{vL}{D} = \frac{10^{-6}\ \text{cm/s} \cdot 0.08\ \text{cm}}{3.4 \times 10^{-6}\ \text{cm}^2/\text{s}} = 0.024$$

indicating that convection is virtually insignificant in the mouse model. Thus, in addition to the physiological differences that complicate scale-up, one must also consider how geometric differences between small and large animals affect drug transport.

ACKNOWLEDGMENTS

This work was supported by the Colorado RNA Center and by NSF grant CCR-9527151. The technical assistance of Corinne Lengsfeld, Daniel McCormick, and Leslie Martien is gratefully acknowledged, as is Radu Serban's help with the COOPT software.

APPENDIX

We present in this Appendix a brief analysis of the diffusion cell shown in Figure 1 of the main article. Of key interest is the effect of lateral diffusion due to the fact that the entire cell surface is not exposed to the source solution. We consider the following diffusion equation for steady diffusion in a radially symmetric cylinder:

$$\frac{1}{r}\frac{\partial}{\partial r}\left(r\frac{\partial c}{\partial r}\right) + \frac{\partial^2 c}{\partial z^2} = 0 \qquad \text{(A1)}$$

The boundary conditions for our problem are

$$c_{z=z_{upper}} = \begin{cases} c_0 & r \le \varepsilon R \\ 0 & \varepsilon R \le r \le R \end{cases}$$

$$c_{z=z_{lower}} = 0$$

$$\left.\frac{\partial c}{\partial r}\right|_{r=0} = \left.\frac{\partial c}{\partial r}\right|_{r=R} = 0 \qquad \text{(A2)}$$

where z_{upper} and z_{lower} are the upper and lower plates, at which the concentration is specified. There is no radial flux at the axis, $r = 0$, by symmetry, and there is no radial flux at the outer edge, $r = R$, because the vessel wall is impenetrable. The radius of the top plate exposed to the solution is given by εR. Multiplying equation (A1) by r and integrating from $r = 0$ to R (equivalent to integrating over a slice of the cell) gives

$$r\frac{\partial c}{\partial r}\Big|_{r=0}^{r=R} + \frac{d^2C}{dz^2} = 0 \qquad \text{(A3)}$$

where C(z) is defined by

$$C(z) \equiv \int_0^K c(r, z)rdr \qquad \text{(A4)}$$

The r-boundary conditions in (A2) require that the first term of (A3) be zero, so we may write

$$\frac{d^2C}{dz^2} = 0 \qquad \text{(A5)}$$

Integrating the z-boundary conditions in (A2) yields boundary conditions on C

$$C|_{z=z_{upper}} = \pi\varepsilon^2R^2c_0$$
$$C|_{z=z_{lower}} = 0 \qquad \text{(A6)}$$

which along with (A5) implies that

$$C = \pi\varepsilon^2R^2c_0\left(\frac{z - z_{lower}}{z_{upper} - z_{lower}}\right) \qquad \text{(A7)}$$

Now, the flux in the z direction, j_z, is given by

$$j_z = -D\frac{\partial c}{\partial z} \qquad \text{(A8)}$$

Integrating this expression to derive the total flow, J_z, gives

$$J_z \equiv \int_0^R j_z rdr = -D\frac{dC}{dz} = -D\left(\frac{\pi\varepsilon^2R^2c_0}{z_{upper} - z_{lower}}\right) \qquad \text{(A9)}$$

The diffusion coefficient may thus be expressed in terms of the flux by

$$D = \frac{-J_zL}{A_{eff}c_0},\ A_{eff} \equiv \rho\varepsilon^2R^2 \qquad \text{(A10)}$$

where A_{eff} is the area exposed to the source solution. It is clear from (A10) that the calculation of D based on the effective area yields the correct value, and that lateral diffusion, although affecting the local concentration profile, does not affect the total mass flow through the cell.

REFERENCES

1. W. M. Hart. *Adler's Physiology of the Eye*, Mosby-Year Book, Chicago, 1992.
2. S. C. Pflugfelder, E. Hernandez, S. J. Fliesler, and J. Alvarez. Intravitreal vancomycin. Retinal toxicity, clearance, and interaction with gentamicin. *Arch. Ophthalmol.* **105**:831–837 (1987).
3. A. Merkli, C. Tabatabay, R. Gurny, and J. Heller. Biodegradable polymers for the controlled release of ocular drugs. *Prog. Poly. Sci.* **23**:563–580 (1998).
4. C. L. Cottriall, N. A. McBrien, R. Annies, and E. M. Leech. Prevention of form-deprivation myopia with pirenzepine: a study of drug delivery and distribution. *Ophthalmic Physiol. Opt.* **19**:327–335 (1999).
5. W. H. Stern, G. P. Lewis, P. A. Erickson, C. J. Guerin, D. H. Anderson, S. K. Fisher, and J. J. O'Donnell. Fluorouracil therapy for proliferative vitreoretinopathy After vitrectomy. *Am. J. Ophthalmol.* **96**:33–42 (1983).
6. Y. Tano, G. Sugita, G. Abrams, and R. Machemer. Inhibition of intraocular proliferations with intravitreal corticosteroids. *Am. J. Ophthalmol.* **89**:131–6 (1980).
7. Y. Nishimura, H. Hayashi, K. Oshima, and S. Iwata. The diffusion in the bovine vitreous. *Acta. Ophthalmol. Jpn.* **90**:1313–6 (1986).
8. R. J. Kaiser and D. M. Maurice. The diffusion of fluorescein in the lens. *Exp. Eye Res.* **3**:156–165 (1964).
9. A. Ohtori and K. J. Toko. In vivo/in vitro correlation of intravitreal delivery of drugs with the help of computer simulation. *Biol. Pharm. Bull.* **17**:283–90 (1994).
10. S. Tsuboi and J. E. Pederson. Volume flow across the isolated retinal pigment epithelium of cynomulgus monkey eyes. *Inv. Ophth. Vis. Sci.* **29**:1652–5 (1988).
11. M. Araie and D. Maurice. The loss of flourescein, flourescein glucuronide and flourescein isothiocyanate dextran from the vitreous by the anterior and retinal pathways. *Exp. Eye Res.* **52**: 27–39 (1991).
12. S. Friedrich, Y. Cheng, and B. Saville. Drug distribution in the vitreous humor of the human eye: the effect of intravitreal injection position and volume. *Cur. Eye Res.* **16**:663–669 (1997).
13. D. L. Epstein, J. M. Hashimoto, P. J. Anderson, and W. M. Grant. Experimental perfusions through the anterior and vitreous chamber with possible relationships to malignant glaucoma. *Am. J. Ophthalmol.* **88**:1078–86 (1979).
14. I. Fatt. Flow and diffusion in the vitreous body of the eye. *Bull. Math. Biol.* **37**:85–90 (1975).
15. D. Maurice. Flow of water between aqueous and vitreous compartments in the rabbit eye. *Am. J. Physiol.* **252**:F104–108 (1987).
16. S. Tsuboi and J. E. Pederson. Effect of plasma osmolality and intraocular pressure on fluid movement across the blood-retinal barrier. *Inv. Ophth. Vis. Sci.* **29**:1747–9 (1988).
17. I. Fatt. Hydraulic flow conductivity of the vitreous gel. *Inv. Ophth. Vis. Sci.* **16**:565–568 (1977).
18. D. M. Knapp, V. H. Barocas, A. G. Moon, K. Yoo, L. R. Petzold, and R. T. Tranquillo. Rheology of reconstituted type I collagen gel in confined compression. *J. Rheology* **41**:971–993 (1997).
19. L. A. Setton, W. Zhu, and V. C. Mow. The biphasic poroviscoelastic behavior of articular cartilage: role of the surface zone in governing the compressive behavior. *J. Biomechanics* **26**:581–592 (1995).
20. F. A. Bettelheim and T. J. Y. Wang. Dynamic viscoelastic properties of bovine vitreous. *Exp. Eye Res.* **23**:435–441 (1976).
21. B. Lee, M. Litt, and G. Buchsbaum. Rheology of the vitreous body: Part 1. Viscoelasticity of human vitreous. *Biorheology* **31**:327–338 (1994).
22. M. Tokita, Y. Fujiya, and K. Hikichi. Dynamic viscoelasticity of the bovine vitreous. *Biorheology* **21**:751–756 (1984).
23. V. H. Barocas and R. T. Tranquillo. An anisotropic biphasic theory of tissue-equivalent mechanics: the interplay among cell traction, fibrillar network deformation, fibril alignment, and cell contact guidance. *J. Biomech. Eng.* **119**:137–145 (1997).
24. M. Dembo and F. Harlow. Cell motion, contractile networks, and the physics of interpenetrating reactive flow. *Biophys. J.* **50**:109–121 (1986).
25. L. Petzold, J. B. Rosen, P. E. Gill, and K. Park. Numerical optimal control of parabolic PDEs using DASOPT. In L. Biegler, *et al.*, (eds.) *Large Scale Optimization with Applications, Part II: Optimal Design and Control, IMA Volumes in Mathematics and its Applications*, Springer-Verlag. New York. 1997, pp. 271–300.
26. C. Geankoplis. *Transport Processes and Unit Operation*, Prentice Hall. New Jersey, 1983.
27. S. P. Chen and H. W. Osterhoudt. Diffusion and solubility of some azo dyes in swollen gelatin matrices—the effects of dye size, matrix swell, and dye matrix interactions. *J. Appl. Poly. Sci.* **30**:2075–2094 (1985).
28. I. Fatt and B. Hedbys. Flow of water in the sclera. *Exp. Eye Res.* **10**:243–249 (1970).
29. W. G. Robison, T. Kuwabara, and J. Zwaan. Eye research. In H. L. Foster, J. D. Small, and J. G. Fox (eds.), *The Mouse in Biomedical Research. Volume IV. Experimental Biology and Oncology*, Academic Press. New York. 1982, p. 69–89.